RESEARCH PAPER

The Effect of TiO_2 Addition on the Microstructure, Crystallization and Dielectric Behavior of BaO-Al_2O_3-SiO_2 Glass System

Farhood Heydari[1], Seyed Mohammad Mirkazemi[1],*, Bijan Eftekhari Yekta[1], Seyyed Salman Seyyed Afghahi[2]

* *mirkazemi@iust.ac.ir*

[1] School of Metallurgy and Materials Engineering, Iran University of Science & Technology (IUST), 1684613114, Tehran, Iran

[2] Department of Materials Science and Engineering, Imam Hossein University, Tehran, Iran

Received: May 2025 **Revised: August 2025** **Accepted: September 2025**

DOI: 10.22068/ijmse.4055

Abstract: *This study investigates the crystallization behavior, phase evolution, and dielectric properties of a BaO-Al_2O_3-SiO_2 glass system modified with 10 wt% TiO_2. Thermal analysis revealed that TiO_2 addition reduced the glass transition temperature from 781.6°C to 779.4°C and the softening point from 838°C to 824.8°C, lowering the calculated nucleation temperature from 810°C to 800°C. Differential thermal analysis indicated sluggish crystallization kinetics, with isothermal heat treatments identifying 1000°C as the optimal processing temperature. This led to the formation of a multiphase crystalline assemblage, including the target monoclinic $Ba_{3.75}Al_{7.5}Si_{8.5}O_{32}$ phase, absent in the TiO_2-free glass, alongside celsian ($BaAl_2Si_2O_8$) polymorphs and barium titanate crystallites, as confirmed by X-ray diffraction. Scanning electron microscopy revealed anisotropic crystal growth with lengths ranging from 1.14 to 1.52 µm. Density measurements using the Archimedes method showed that the titanium-containing glass had a density of 3.35 g/cm³, which increased to 3.85 g/cm³ after heat treatment at 1000°C for 48 hours. Dielectric characterization in the Ku-band (12.4–18 GHz) demonstrated enhanced properties, with the relative permittivity decreasing from 10.40 to 6.38 and the dielectric loss tangent improving from 0.3 to 0.2 post-crystallization. These enhancements, driven by the tailored crystalline phase assemblage facilitated by TiO_2, position this glass-ceramic system as a promising candidate for high-frequency microwave applications requiring low dielectric loss and stability. The role of TiO_2 as an effective crystallization modifier is highlighted, enabling optimized dielectric performance through controlled devitrification and targeted phase formation.*

Keywords: *Barium aluminosilicate glass-ceramics, Controlled crystallization, Ku-band dielectric constant, Dielectric loss tangent.*

1. INTRODUCTION

Barium aluminosilicate (BAS) glass-ceramics are valued for their unique properties, including low thermal expansion, high mechanical strength, and excellent dielectric performance, driven by their crystalline phases: hexagonal, monoclinic, and orthorhombic structures [1-3]. The monoclinic celsian phase, with a thermal expansion coefficient of ~2.3×10^{-6} K^{-1}, is thermodynamically stable, whereas the hexagonal hexacelsian (~8.0×10^{-6} K^{-1}) and orthorhombic α-hexacelsian phases are metastable, often forming preferentially during sintering below 1590°C [1, 4-6]. The hexacelsian-to-celsian (H-M) transformation faces a significant kinetic barrier [7-11], and the reversible transition between hexacelsian and α-hexacelsian near 300°C induces a ~3% volume change, leading to microcracking and potential material failure [12]. These challenges have prompted extensive research to promote the stable celsian phase in BAS glass-ceramics [7-9]. Strategies to control crystallization include the use of nucleating agents like ZrO_2 [13] and mineralizers such as Li_2O [14-18], LiF, Na_2O [19], and CaO [20, 21]. While these additives reduce glass viscosity to facilitate celsian formation [22, 23], they often require high-temperature processing or compromise the thermal stability of the BAS network. Titanium dioxide (TiO_2) stands out as a promising additive due to its dual role: as a nucleating agent, it lowers the activation energy for crystallization, and as a network modifier, it enhances glass-forming ability [2, 3, 24]. The selection of 10 wt% TiO_2 in this study was based on prior research, such as Li et al. [26], which identified TiO_2 concentrations between 8–16 wt% as optimal for enhancing crystallization behavior and dielectric properties in similar glass systems (e.g., CaO-Al_2O_3-SiO_2). Specifically, 10 wt% TiO_2 was chosen as it provides a balance between reducing the activation energy for crystallization and minimizing excessive phase separation or precipitation of undesirable titanium oxide phases, which could

[DOI: 10.22068/ijmse.4055]

compromise material properties. Preliminary experiments confirmed that lower concentrations (e.g., 5 wt%) had a limited impact on the formation of the desired monoclinic $Ba_{3.75}Al_{7.5}Si_{8.5}O_{32}$ phase, while higher concentrations (e.g., 15 wt%) promoted excessive phase separation.

The targeted application of the optimized glass-ceramic in this study is the development of low-loss dielectric materials for high-frequency microwave applications, such as telecommunications antennas, radio frequency (RF) filters, and integrated circuit substrates for 5G and beyond. The incorporation of 10 wt% TiO_2 facilitates the formation of the monoclinic $Ba_{3.75}Al_{7.5}Si_{8.5}O_{32}$ phase and celsian polymorphs, which exhibit a low dielectric constant (reduced from 10.40 to 6.38) and improved loss tangent (from 0.3 to 0.2) in the Ku-band (12.4–18 GHz), making them ideal for rapid wave propagation and minimal energy loss. Additionally, the enhanced thermal stability and mechanical integrity due to the controlled crystalline microstructure render this glass-ceramic suitable for applications such as microwave-transparent radome coatings, which require both dielectric performance and mechanical robustness. Despite these advancements, the crystallization behavior, phase evolution, and dielectric properties of BAS glasses with 10 wt% TiO_2 remain underexplored. This study systematically investigates the effects of TiO_2 on characteristic temperatures (glass transition, softening, and crystallization), phase formation pathways, and microstructural development, with a focus on correlating processing conditions with crystalline phase distribution and dielectric performance. The findings offer insights into tailoring BAS glass-ceramics for high-frequency applications and validate the adaptation of TiO_2 concentration guidelines from related glass systems [26]. Future research will explore a wider range of TiO_2 concentrations (5–15 wt%) to fully elucidate composition-property relationships in this material system.

2. EXPERIMENTAL PROCEDURES

High-purity raw materials—alumina (Al_2O_3, 99.99%), barium carbonate ($BaCO_3$, 99.95%), silica (SiO_2, 99.9%), and titanium dioxide (TiO_2, 99.8%)—were weighed in proportions of 10, 35, 55, and 10 wt%, respectively, to prepare the BaO-Al_2O_3-SiO_2-TiO_2 glass system. These materials were blended in a planetary ball mill with alumina balls for 4 hours in an ethanol medium to achieve uniform homogenization, followed by drying at 80°C for 12 hours to remove residual ethanol. The dried mixture was placed in alumina crucibles and melted in an electric furnace at 1600°C for 2 hours with a heating rate of 10°C/min. The molten glass was quenched in water to form a glass matrix and then cast into stainless steel molds preheated to 600°C. Immediately after casting (within 15–20 seconds), the molds containing the samples were transferred to a furnace set at 600°C for annealing. The furnace was then turned off, allowing the samples to cool naturally to room temperature (25°C) over approximately 4–5 hours to minimize thermal stresses and ensure structural integrity. Fourier transform infrared (FTIR) spectroscopy (Shimadzu 8400S) was conducted on powdered samples in the 400–4000 cm^{-1} range to analyze molecular structure. Thermal properties were evaluated using dilatometry (Bähr Thermo Analyze DIL 801 L, Germany; heating rate: 5°C/min) and differential thermal analysis (DTA) (Bähr Thermo Analyze STA 503, Germany; heating rate: 0.01–100°C/min). Crystalline phases were identified by X-ray diffraction (XRD) using a Philips X'Pert diffractometer with CuKα radiation. Microstructural analysis was performed via scanning electron microscopy (SEM) (Nova Nano SEM 200, FEI Company) equipped with energy-dispersive X-ray spectroscopy (EDS). Sample density was determined using the Archimedes method. For dielectric characterization, glass and glass-ceramic samples were prepared as rectangular specimens with a length of 15.7 mm, a width of 7.9 mm, and a thickness of 2 mm. The samples were cut using a micro-cutter with a C-BN coating and subsequently ground using a rotating wheel with a C-BN coating to achieve precise final dimensions. Dielectric properties were measured in the 12.4–18 GHz frequency range (Ku-band) using a Keysight E5063A vector network analyzer. The samples were placed in a rectangular waveguide, and the transmission/reflection method was employed to calculate the relative permittivity (ε_r) and dielectric loss tangent ($\tan\delta$). Measurements were conducted at room temperature (25°C) under controlled humidity (< 50%) to minimize environmental effects. The analyzer was calibrated using known standards (air and PTFE) to ensure measurement accuracy.

[DOI: 10.22068/ijmse.4055]

3. RESULTS AND DISCUSSION

3.1. FTIR Characterization

FTIR analysis was done to investigate the role of Titania in the structure of $BaO\text{-}Al_2O_3\text{-}SiO_2$ glass, and the resulting curves are shown in Figure 1.

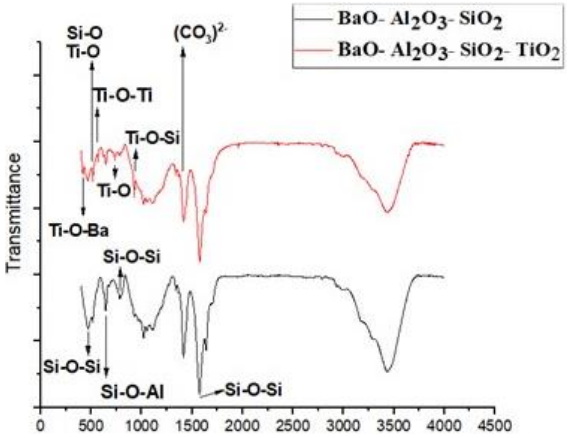

Fig. 1. FTIR curve related to the base glass and glass containing titania

FTIR analysis of $BaO\text{-}Al_2O_2\text{-}SiO_2$ and $BaO\text{-}Al_2O_3\text{-}SiO_2\text{-}TiO_2$ glass systems revealed distinct molecular structures. Peaks corresponding to Si–O and Si–O–Si bonds in both compositions confirm the presence of symmetric $(SiO_4)^{4-}$ tetrahedra with bridging oxygens, forming the core silicate network. Si–O–Al peaks indicate an aluminosilicate tetrahedral structure in both systems. In the $BaO\text{-}Al_2O_3\text{-}SiO_2\text{-}TiO_2$ glass, the emergence of Ti–O and Ti–O–Ti peaks underscores the network-modifying role of TiO_2. Ti^{4+} ions disrupt Si–O–Si bonds, forming weaker Ti–O linkages and occupying interstitial sites within the silicate matrix [28]. This disruption occurs through a two-stage process: initially, oxygen atoms are drawn toward Ti^{4+} ions, elongating three Si–O bonds and contracting the fourth, thus transforming symmetric SiO_4 tetrahedra into asymmetric configurations. Subsequently, the weakened Si–O bond breaks, producing trigonal pyramidal SiO_3 units with non-bridging oxygens [29]. The presence of Ti–O–Si and Ti–O peaks indicates the incorporation of TiO_2 into the glass network as $(TiO_4)^{4-}$ units, while Ti–O–Ti peaks suggest partial segregation of Ti^{4+} ions, stabilizing octahedral $(TiO_6)^{8-}$ units at lower temperatures [24]. These structural changes indicate that TiO_2 acts as a network modifier, reducing the activation energy for crystallization and facilitating the formation of crystalline phases, as observed in subsequent XRD and SEM analyses. The peak at 420 cm^{-1}, absent in the base glass, suggests interactions involving Ti^{4+} ions within the glass matrix, contributing to the modification of the silicate network. The reduced intensity of Si–O–Si and Si–O–Al peaks in the TiO_2-containing glass compared to the base $BaO\text{-}Al_2O_3\text{-}SiO_2$ system reflects the replacement of some Si–O–Si and Si–O–Al bonds with Ti–O linkages, further evidencing TiO_2's role as a network modifier.

3.2. Thermal-Physical Properties of Glasses

Dilatometric analysis compared the $BaO\text{-}Al_2O_3\text{-}SiO_2\text{-}TiO_2$ glass system (with 10 wt% TiO_2) to the pure $BaO\text{-}Al_2O_2\text{-}SiO_3$ glass, as shown in Figure 2A.

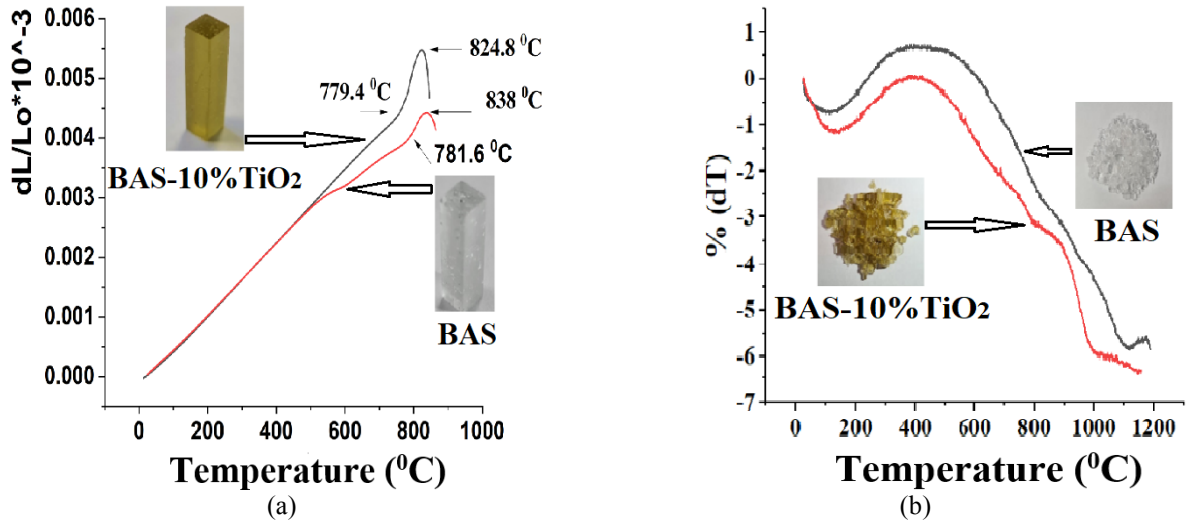

Fig. 2. Thermal-physical properties of BAS, BAS- 10% TiO_2 a) Dilatometric, b) DTA

[DOI: 10.22068/ijmse.4055]

The addition of TiO_2 slightly lowered the glass transition temperature (Tg) from 781.6°C to 779.4°C and significantly reduced the softening temperature (Ts) from 838°C to 824.8°C. Consequently, the nucleation temperature, calculated as (Tg+Ts)/2 [30], decreased from 810°C to 800°C in the TiO_2-modified system. Differential thermal analysis (DTA) of the TiO_2-containing glass revealed no distinct crystallization peaks (Figure 2B), indicating sluggish crystallization kinetics likely due to the high viscosity of the glass matrix. However, TiO_2 acts as a network modifier, reducing the activation energy for crystallization, as evidenced by the lower nucleation temperature (800°C vs. 810°C in the pure system) [24, 29]. This effect is attributed to the disruption of Si–O–Si bonds by Ti^{4+} ions, promoting the formation of weaker Ti–O linkages (Figure 1) and thereby lowering the energy barrier for nucleation and crystal growth. Due to the lack of well-defined crystallization peaks in the DTA curves, quantitative kinetic analysis (e.g., Kissinger or Ozawa methods) was not feasible. Future studies will employ variable heating rate DTA to determine the activation energy of crystallization, providing further insight into the kinetic behavior of the TiO_2-modified BAS system. To investigate crystallization behavior in the absence of clear exothermic events, isothermal heat treatments were conducted. Stepwise heating with 50°C increments and 1-hour holds was performed, starting at the nucleation temperature of 800°C. The optimal processing temperature was determined to be 1000°C, as visible deformation occurred at 1050°C. Crystallization studies were thus carried out at 1000°C for durations ranging from 4 to 48 hours to systematically evaluate phase evolution in the TiO_2-modified system.

3.3. XRD Analysis of Heat-Treated Samples

X-ray diffraction analysis of both pure BaO-Al_2O_3-SiO_2 (BAS) and BAS glass systems with added titania (TiO_2) demonstrates the critical role of TiO_2 in facilitating crystallization, with particular efficacy in nucleating the technologically significant monoclinic $Ba_{3.75}Al_{7.5}Si_{8.5}O_{32}$ phase (Figure 3). The pure BAS system exhibited limited crystallizability, showing no detectable phases after 4-8 hours of heat treatment. After 12 hours, only $BaAl_2Si_2O_8$ crystallized in hexagonal and orthrohombic forms, with prolonged treatment to 36 hours increasing their concentration. At 48 hours, monoclinic $BaSi_2O_5$ appeared, while the desired $Ba_{3.75}Al_{7.5}Si_{8.5}O_{32}$ phase remained absent throughout all treatment durations. In striking contrast, the TiO_2-modified system demonstrated significantly enhanced crystallization behavior. While similarly showing no crystallization after 4-8 hours, three distinct phases emerged after 12 hours: $BaAl_2Si_2O_8$ (hexagonal/orthorhombic), the target $Ba_{3.75}Al_{7.5}Si_{8.5}O_{32}$ (monoclinic) phase, and $Ba_2Ti_6O_{13}$ (monoclinic). Progressive intensification of all crystalline peaks occurred at 36-48 hours, particularly for the $Ba_{3.75}Al_{7.5}Si_{8.5}O_{32}$ phase. The preferential precipitation of the monoclinic $Ba_{3.75}Al_{7.}5Si_{8.5}O_{32}$ phase in the TiO_2-modified system is attributed to multiple synergistic mechanisms driven by TiO_2. Firstly, the high field strength of Ti^{4+} ions disrupts the Si–O–Si bonds within the glass network (Figure 1), forming weaker Ti–O linkages that lower the activation energy for crystallization, as evidenced by the reduced nucleation temperature (from 810°C to 800°C) [28, 29].

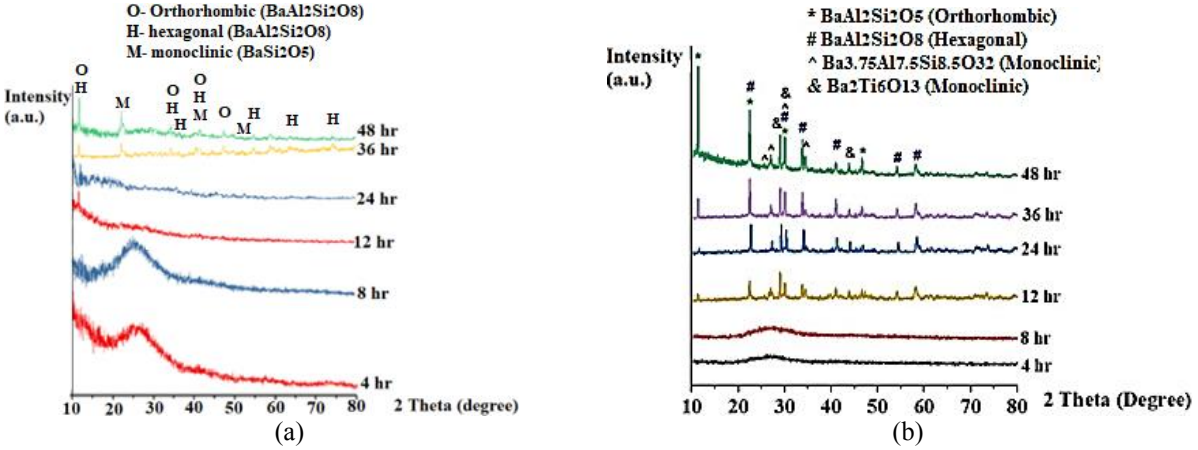

Fig. 3. X-ray diffraction pattern of heat-treated glasses a) BaO- Al_2O_3- SiO_2, b) BaO- Al_2O_3-SiO_2- TiO_2

[DOI: 10.22068/ijmse.4055]

This structural modification facilitates the nucleation of crystalline phases, including $Ba_{3.75}Al_{7.5}Si_{8.5}O_{32}$. Secondly, TiO_2 creates titanium-rich regions within the glass matrix, which serve as favorable nucleation sites for the target phase due to local compositional and structural compatibility [24]. These regions, characterized by $(TiO_6)^{8-}$ octahedral units (Figure 1), may act as structural templates that promote the formation of the monoclinic $Ba_{3.75}Al_{7.5}Si_{8.5}O_{32}$ phase. Thirdly, TiO_2 alters the crystallization pathway, suppressing the formation of undesirable phases like hexacelsian, which dominates in the pure BAS system, and instead promoting the target phase, as observed after 12 hours of heat treatment at 1000°C. Additionally, the formation of transient barium titanate crystallites ($Ba_2Ti_6O_{13}$) likely serves as an intermediate phase that further catalyzes the nucleation of $Ba_{3.75}Al_{7.5}Si_{8.5}O_{32}$ by providing chemically and structurally compatible interfaces. These combined effects highlight TiO_2's critical role as both a nucleation catalyst and a phase selector, enabling the controlled formation of the desired $Ba_{3.75}Al_{7.5}Si_{8.5}O_{32}$ phase, which is absent in the pure BAS system under identical conditions.

3.4. SEM Microstructural Characterization of Heat-Treated Samples

The scanning electron micrographs in Figure 4(a-d) (10,000× magnification) illustrate the microstructural evolution of BAS-10%TiO_2 glass-ceramics subjected to a two-stage heat treatment process consisting of nucleation at 800°C for 4 hours followed by crystal growth at 1000°C for durations ranging from 12 to 48 hours.

Heat treatment time	Sample heat treated	SEM micrographs
12 hr		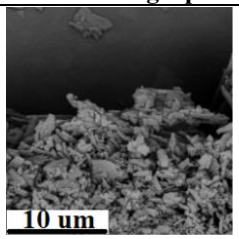 (a)
24 hr		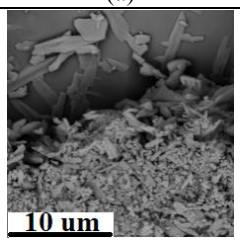 (b)
36 hr		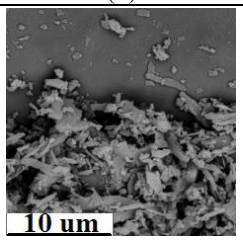 (c)
48 hr		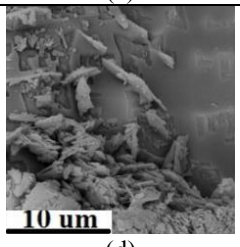 (d)

Fig. 4. Images of the glass containing 10% by weight of titania, heat-treated at 800°C for 4 hours and subsequently at 1000°C for a) 12, b) 24, c) 36, and d) 48 hours, are presented

[DOI: 10.22068/ijmse.4055]

The microstructural development exhibits a clear correlation between heat treatment duration and crystallized layer thickness, demonstrating progressive microstructural coarsening with increased processing time. The crystallized matrix reveals a uniform distribution of crystalline phases displaying distinct morphological features, including both equiaxed grains and anisotropic rod-shaped crystals Figure 4(a-d). Extended crystallization periods promote the development of dendritic growth patterns, where primary dendrites nucleate and propagated into the bulk material. The initial unconstrained dendritic growth transitions to a confined growth regime as neighboring dendrites interact, ultimately forming an interconnected interdendritic network characteristic of advanced crystallization stages Figure 4(a-d).

This microstructural evolution suggests a transition from interface-controlled to diffusion-limited crystallization kinetics, consistent with classical glass-ceramic systems where isothermal heat treatment parameters directly influence phase development and morphological characteristics.

Quantitative EDS analysis (Figure 5(b-c)) reveals significant compositional gradients between microstructural constituents: aluminum content increases from 9.56 at% in interdendritic glassy regions to 22.67 at% in adjacent dendritic zones, while silicon decreases from 35.04 at% to 19.37 at%. Concurrently, barium concentration rises from 11.05 at% to 14.16 at%, indicating substantial elemental redistribution during crystallization.

The strong field strength of Ti^{4+} ions enhances heterogeneous nucleation kinetics, facilitating the formation of crystalline phases such as $Ba_{3.75}Al_{7.5}Si_{8.5}O_{32}$, as confirmed by XRD analysis. While TiO_2 is known to promote phase separation in glass-ceramic systems [29], direct evidence of phase separation (e.g., through dedicated SEM micrographs) was not obtained in this study due to experimental constraints. Instead, the observed compositional gradients and crystalline phase development suggest that TiO_2 primarily acts as a nucleation catalyst, lowering the activation energy for crystallization. Future studies will include detailed SEM analysis to directly investigate phase separation phenomena. A more detailed analysis of the microstructure using ImageJ software reveals that the size of the crystalline phases increases proportionally with longer heat treatment durations (Figure 6). However, the average size of the crystalline phases remains relatively unchanged. This suggests that titania is an effective additive for producing fine-grained glass-ceramics, consistent with findings reported by other researchers [12, 13]. One of the key advantages of such a microstructure is its contribution to enhanced strength and toughness in glass-ceramics [33].

3.5. Dielectric Characterization of the Samples

Based on the obtained results, the sample heat-treated for 48 hours, which contained the highest amount of crystallized phase, was selected as the optimal sample, and its transparency against microwaves was tested in the Ku frequency range (12.4–18 GHz). The dielectric properties, including permittivity and dielectric loss tangent, were evaluated for both the BAS-10%TiO_2 glass and the BAS-10%TiO_2-48hr glass-ceramic samples, as shown in Figure 7. The test results indicate that the average dielectric constant of the glass sample was 10.40, while that of the glass-ceramic sample was 6.38.

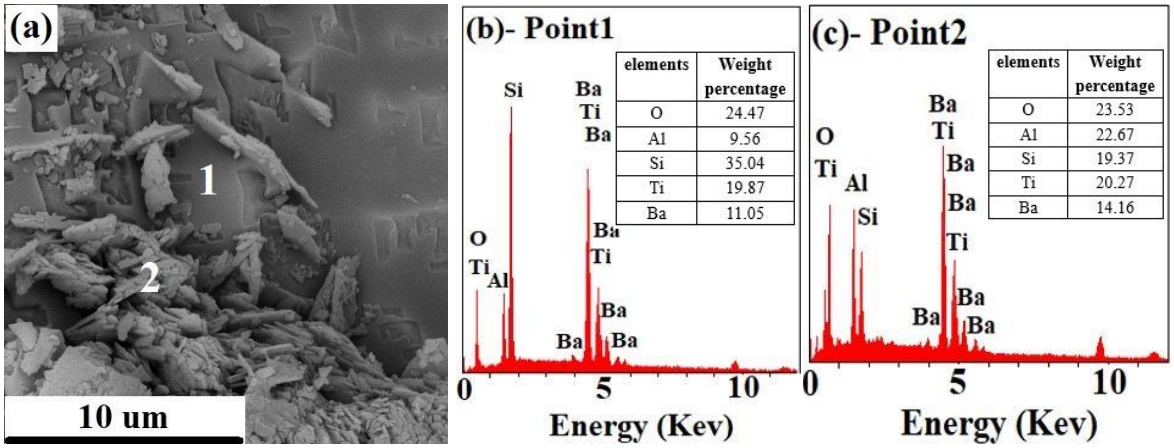

Fig. 5. Electron microscope image and elemental analysis of sample BAS- 10% TiO_2- 48 hr

[DOI: 10.22068/ijmse.4055]

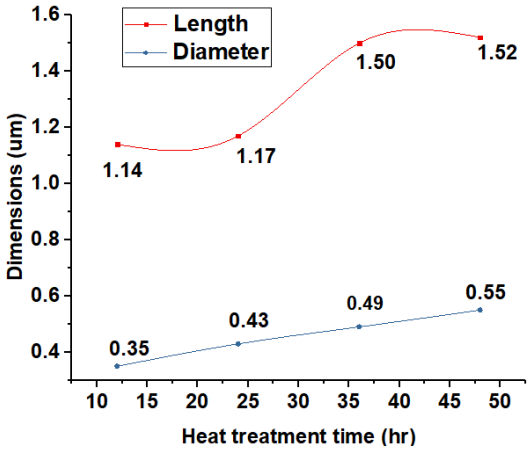

Fig. 6. Changes in the length and diameter of rod grains in the structure with the change of heat treatment time in BAS-10% TiO_2 sampl

Similarly, the average dielectric loss tangent (tan δ) of the glass sample was 0.3, compared to 0.2 for the glass-ceramic sample. This stability in dielectric loss, along with the potential improvement in mechanical properties resulting from crystallization, makes this glass-ceramic composite suitable for applications requiring both mechanical strength and telecommunication performance. The dielectric constant and dielectric loss are influenced by factors such as the type and amount of crystalline and glass phases, dielectric polarizability of components (α), porosity, and density [34]. The relationship between dielectric constant and frequency depends on factors such as the type and number of charge carriers, electrode polarization, and space charge [35]. A low dielectric constant facilitates rapid wave propagation, while reduced dielectric loss minimizes wave attenuation and heat generation, particularly at high frequencies [36]. The sum of intrinsic and extrinsic losses determines the dielectric losses in the samples. Intrinsic losses arise from interactions between phonons and the incident electric field, which are influenced by the material's crystal structure [36]. The frequency independence of the dielectric constant in the microwave range is consistent with the damped harmonic oscillator model, which predicts that the frequency of microwave waves is significantly lower than that of phonons [37]. In real-world samples, there are always defects that disrupt the ideal harmonic oscillator model [36]. On the other hand, extrinsic losses result from energy dissipation caused by secondary phases (crystalline and glass phases), porosity, microcracks, interfaces, and crystal defects [38]. Density measurements using the Archimedes method showed that the BAS-10%TiO_2 glass had a density of 3.35 g/cm^3, which increased to 3.85 g/cm^3 after heat treatment (48 hours at 1000°C), corresponding to an approximate 14.9% increase in density. This densification indicates a significant reduction in porosity due to the crystallization process, which, combined with the formation of low-loss crystalline phases such as celsian (tan δ≈ 0.007 [39]) and $Ba_{3.75}Al_{7.5}Si_{8.5}O_{32}$, contributes to the observed reduction in dielectric loss tangent from 0.3 to 0.2 in the glass-ceramic sample. To further quantify the impact of porosity on dielectric performance, future studies will include detailed measurements of porosity volume percentage using the Archimedes method to establish a precise correlation with dielectric properties. Frequency, resonance, and quality factor (Q-factor) were not measured in this study due to the focus on characterizing permittivity and dielectric loss tangent using the transmission/ reflection method with a Keysight E5063A vector network analyzer.

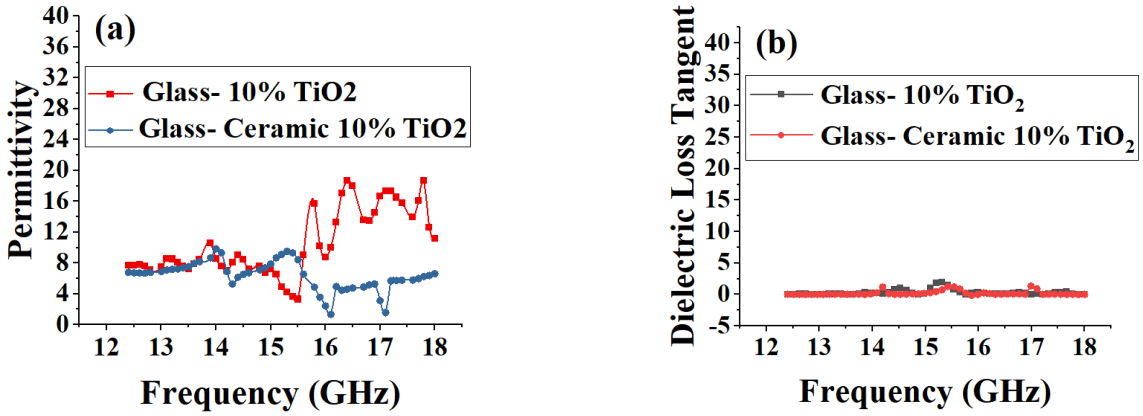

Fig. 7. Frequency-dependent variations of a) relative permittivity (ε_r) and b) dielectric loss tangent (tan δ) in the Ku-band (12.4–18 GHz) for: BAS-10%TiO_2 glass and BAS-10%TiO_2 glass-ceramic (heat-treated for 48 h)

[DOI: 10.22068/ijmse.4055]

These parameters are critical for applications such as resonators and filters in high-frequency systems. Future studies will incorporate advanced measurement techniques, such as cavity resonator methods, to determine the resonance frequency and quality factor, providing a more comprehensive evaluation of the dielectric performance of the BAS-10%TiO_2 glass-ceramic system.

4. CONCLUSIONS

Thermal characterization of the BaO-Al_2O_3-SiO_2-TiO_2 glass system revealed a significant reduction in characteristic temperatures compared to the TiO_2-free baseline glass. The incorporation of 10 wt% TiO_2 lowered both the glass transition temperature and softening point, consequently decreasing the calculated nucleation temperature. While thermal analysis indicated sluggish crystallization kinetics, isothermal heat treatments established 1000°C as the upper processing limit, leading to the formation of a multiphase crystalline assemblage. X-ray diffraction confirmed that the TiO_2-modified system developed a targeted monoclinic $Ba_{3.75}Al_{7.5}Si_{8.5}O_{32}$ phase—absent in the TiO□-free glass even after prolonged heat treatment-alongside celsian ($BaAl_2Si_2O_8$) polymorphs and barium titanate crystallites, collectively enhancing the material's properties. Microstructural evolution exhibited anisotropic growth, contributing to a refined grain distribution. The resulting glass-ceramic demonstrated superior dielectric performance in the microwave frequency regime, with reduced relative permittivity and improved loss tangent. These improvements are attributed to the tailored crystalline phase assemblage, particularly the $Ba_{3.75}Al_{7.5}Si_{8.5}O_{32}$ phase, and the controlled microstructure enabled by TiO_2 addition. Although mechanical properties such as hardness and fracture toughness were not directly measured due to experimental constraints, the fine-grained microstructure and uniform phase distribution—including $Ba_{3.75}Al_{7.5}Si_{8.5}O_{32}$ and celsian polymorphs—suggest enhanced mechanical integrity compared to the amorphous glass. Prior studies [12, 33] support that glass-ceramics with dense crystalline structures and minimal porosity, as observed in SEM analysis, typically exhibit higher hardness and fracture toughness. Future work will include mechanical testing (e.g., Vickers hardness and fracture toughness measurements) to quantitatively evaluate this system's suitability for high-frequency applications requiring both dielectric and mechanical robustness. These findings highlight TiO_2's efficacy as a crystallization modifier, facilitating the development of BAS glass-ceramics with optimized dielectric properties through controlled devitrification and strategic phase formation.

REFERENCES

[1] Yoshiki, K. M., "High-temperature modification of barium feldspar". J. Am. Ceram. Soc., 1951, 34, 283-286.

[2] Lin, H. C. and Lin, W. R. F., "Studies in the system BaO-Al_2O_3-SiO_2: V. The ternary system sanbornite-celsian-silica". J. Am. Ceram. Soc., 1970, 53, 549-551.

[3] Martínez-López, R., "Chemical interaction between Ba-celsian ($BaAl_2Si_2O_8$) and molten aluminum". Ceram. Int., 2016, 42, 3491-3496.

[4] Han, M., Wang, X. Y., Li, M., "Effect of strontium doping on dielectric and infrared emission properties of barium aluminosilicate ceramics". Mater. Lett., 2016, 183, 223-226.

[5] Lin, H. C. and Lin, W. R. F., "Studies in the system BaO-Al_2O_3-SiO_2: I. The polymorphism of celsian". Am. Mineral. J. Earth Planet. Mater., 1968, 53, 134-144.

[6] Semler, C. E. and Lin, W. R. F., "Studies in the system BaO-Al□O□-SiO□: IV. The system celsian-alumina and the join celsian-mullite". J. Am. Ceram. Soc., 1969, 52, 679-680.

[7] He, P., Fu, J. C., Wang, M., Wang, R., Yuan, J. and Jia, D., "Monoclinic-celsian ceramics formation: through thermal treatment of ion-exchanged 3D printing geopolymer precursor". J. Eur. Ceram. Soc., 2019, 39, 563-573.

[8] Marocco, M. P., Antonello., Dell'Agli, G., Spiridigliozzi, L. and Esposito, S., "The multifarious aspects of the thermal conversion of Ba-exchanged zeolite A to monoclinic celsian". Microporous Mesoporous Mater., 2018, 256, 235-250.

[9] Biesuz, M. P., Marocco, A., Spiridigliozzi, L., Dell'Agli, G. and Sglavo, V. M., "Sintering behavior of Ba/Sr celsian precursor obtained from zeolite-A by ion-exchange method". J. Am. Ceram. Soc.,

[DOI: 10.22068/ijmse.4055]

2017, 100, 5433-5443.
[10] López-Badillo, C. M., López-Cuevas, J., Gutiérrez-Chavarría, C. A., Rodríguez-Galicia, J. L. and Pech-Canul, M. I., "Synthesis and characterization of $BaAl_2Si_2O_8$ using mechanically activated precursor mixtures containing coal fly ash". J. Eur. Ceram. Soc., 2013, 33, 3287-3300.
[11] Ma, M. T., Zhu, D., Zhao, C., Han, T. and Cao, S., "Effect of Sr^{2+}-doping on structure and luminescence properties of $BaAl_2Si_2O_8$: Eu² phosphors". Opt. Commun., 2012, 285, 665-668.
[12] Bandyopadhyay, O. B. C., Aswath, P. B. and Porter, W. D., "The low temperature hexagonal to orthorhombic transformation in Si_3N_4 reinforced BAS matrix composites". J. Mater. Res., 1995, 10, 1256-1263.
[13] Debsikdar, O. S. S. and Lee, W. E., "Effect of zirconia addition on crystallinity, hardness, and microstructure of gel-derived barium aluminosilicate, $BaAl_2Si_2O_8$". J. Mater. Sci., 1992, 27, 5320-5324.
[14] Khater, G. A. and Idris, M. H., "Role of TiO_2 and ZrO_2 on crystallizing phases and microstructure in Li, Ba aluminosilicate glass". Ceram. Int., 2007, 33, 233-238.
[15] Ferone, M. P., Esposito, S. and Dell'Agli, G., "Role of Li in the low temperature synthesis of monoclinic celsian from (Ba, Li)-exchanged zeolite-A precursor". Solid State Sci., 2005, 7, 1406–1414.
[16] Lee, W. E., Chen, M. and James, P. F., "Crystallization of celsian ($BaAl_2Si_2O_8$) glass". J. Am. Ceram. Soc., 1995, 78, 2180-2186.
[17] Wu, S., Xia, L., Shi, B. and Wen, G., "Microscopic scale evidence of phase transformation process in barium aluminosilicate glass-ceramic". J. Eur. Ceram. Soc., 2018, 38, 727-733.
[18] Debsikdar, J. C., "Gel to glass conversion and crystallization of alkoxy-derived barium aluminosilicate gel". J. Non-Cryst. Solids, 1992, 144, 269-276.
[19] Shao, J. L., Hu, X., Zhao, Y., Chen, S., Liu, L. and Chen, J., "Crystallization and dielectric properties of oxyfluoride aluminosilicate glasses added with Na_2O". J. Non-Cryst. Solids, 2022, 576, 121277.
[20] Oliveira, J. M. F. and Lee, W. E., "Structural and mechanical characterisation of MgO-, CaO- and BaO-doped aluminosilicate ceramics". Mater. Sci. Eng. A, 2003, 344, 35-44.
[21] Lee, K. T. and Aswath, P. B., "Kinetics of the hexacelsian to celsian transformation in barium aluminosilicates doped with CaO". Int. J. Inorg. Mater., 2001, 3, 687-692.
[22] Bošković, S., Kosanović, Đ., Bahloul-Hourlier, D., Thomas, P. and Kiss, S., "Formation of celsian from mechanically activated $BaCO_3$–Al_2O_3–SiO_2 mixtures". J. Alloys Compd., 1999, 290, 230-235.
[23] Ye, M. I. and Chen, S., "Synthesis and properties of barium aluminosilicate glass–ceramic composites reinforced with in situ grown Si_3N_4 whiskers". Scr. Mater., 2003, 48, 1433-1438.
[24] Zhu, W., Jiang, H., Sun, S., Jia, S. and Liu, Y., "Effect of TiO_2 content on the crystallization behavior and properties of CaO-Al_2O_3-SiO_2 glass ceramic fillers for high temperature joining application". J. Alloys Compd., 2018, 732, 141-148.
[25] Shelby, J. E., Introduction to glass science and technology. Cambridge: Royal Society of Chemistry, 1997.
[26] Li, F. and Liu, X., "Effect TiO_2 of made of ash fly on crystallization activation energy and index". Proceedings of the MATEC Web Conference, 2015, 01008.
[27] Ma, M., Ni, W., Wang, Y., Wang, Z. and Liu, F., "The effect of TiO_2 on phase separation and crystallization of glass-ceramics in CaO–MgO–Al_2O_3–SiO_2–Na_2O system". J. Non-Cryst. Solids, 2008, 354, 5395-5401.
[28] Mostafa, A. G. and El-Hadi, Z. A., "Effect of Pb ions on the ionic conductivity of some silicate glass systems". J. Mater. Sci. Mater. Electron., 2002, 18, 391-394.
[29] Reben, M., Kosmal, M., Ziąbka, M., Pichniarczyk, P. and Grelowska, I., "The influence of TiO_2 and ZrO_2 on microstructure and crystallization behavior of CRT glass". J. Non-Cryst. Solids, 2015, 425, 118-123.
[30] Upadhyaya, G. S., Glass-ceramic technology. Westerville, OH: The American Ceramic Society, 2002.
[31] Wisniewski, W., Carl, R. and Rüssel, C., "Complex growth structures of mullite after electrochemically induced nucleation".

[DOI: 10.22068/ijmse.4055]

Cryst. Eng. Comm., 2014, 16, 1192–1200.
[32] Doherty, P. E., Lee, D. W. and Davis, R. S., "Direct observation of the crystallization of Li_2O-Al_2O_3-SiO_2 glasses containing TiO_2". J. Am. Ceram. Soc., 1967, 50, 77-81.
[33] Theocharopoulos, A., Chen, X., Wilson, R. M., Hill, R. and Cattell, M. J., "Crystallization of high-strength nano-scale leucite glass-ceramics". Dent. Mater., 2013, 29, 1149-1157.
[34] Hsiang, H. I., Chen, C. C. and Yang, S. Y., "Structure, crystallization, and dielectric properties of the Al_2O_3 filled CaO–B_2O_3–SiO_2–Al_2O_3 glass composites for LTCC applications". Jpn. J. Appl. Phys., 2019, 58, 091010.
[35] Haily, E., Bih, L., Jerroudi, M., Yousfi, S. and Manoun, B., "Structural and dielectric properties of K_2O-TiO_2-P_2O_5 glass and its associated glass-ceramic". Mater. Today Proc., 2020, 30, 849-853.
[36] Wang, S. F., Lai, B. C., Hsu, Y. F. and Lu, C. A., "Dielectric properties of CaO–B_2O_3–SiO_2 glass-ceramic systems in the millimeter-wave frequency range of 20–60 GHz". Ceram. Int., 2021, 47, 22627-22635.
[37] Szwagierczak, D., Synkiewicz-Musialska, B., Kulawik, J., Czerwińska, E., Pałka, N. and Bajurko, P. R., "Low temperature sintering of $Zn_4B_6O_{13}$ based substrates, their microstructure and dielectric properties up to the THz range". J. Alloys Compd., 2020, 819, 153025.
[38] Yu, H., Liu, J., Zhang, W. and Zhang, S., "Ultra-low sintering temperature ceramics for LTCC applications: a review". J. Mater. Sci. Mater. Electron., 2015, 26, 9414-9423.
[39] Borhan, A. I., Gromada, M., Nedelcu, G. G. and Leontie, L., "Influence of (CoO, CaO, B_2O_3) additives on thermal and dielectric properties of BaO–Al_2O_3–SiO_2 glass–ceramic sealant for OTM applications". Ceram. Int., 2016, 42, 10459-10468.

[DOI: 10.22068/ijmse.4055]